A bio-inspired micro-structured surface with anisotropic adhesion

Luciano Afferrante*, Francesco Bottiglione, Elena Pierro and Giuseppe Carbone

Department of Mechanics, Mathematics and Management (DMMM), Politecnico di Bari,
Viale Japigia, 185 Bari, Italy
*Corresponding author: l.afferrante@poliba.it

1. Introduction

Micro-patterned surfaces, inspired by the observation of natural systems [1], have been drawing a strong scientific interest as a consequence of their enhanced adhesive [2-6], or superhydrorepellent [7] properties. Because of their relevance in (i) medical adhesive bands [8, 9], (ii) gecko inspired robots [10, 11], (iii) gecko tires [12], (iv) adhesive gloves and suits [13], several efforts have been made to fabricate fibrillar surfaces which may replicate the adhesive properties of geckos and insects [14-17]. The amazing adhesion of such man-made biomimetic surfaces has been considered as a sort of magic, until very recent studies have shed light on the fundamental physical mechanisms providing their micro- and nano-structured surfaces with optimized adhesive properties [5, 6]. However, often these systems shown almost perfect isotropic adhesive properties which do not perfectly fit those engineering applications, (e.g. robot-locomotion and object manipulation) where enhanced adhesion is desired for loading in one direction, and no enhancement or a reduction in adhesion is desired along other directions to facilitate system detachment.

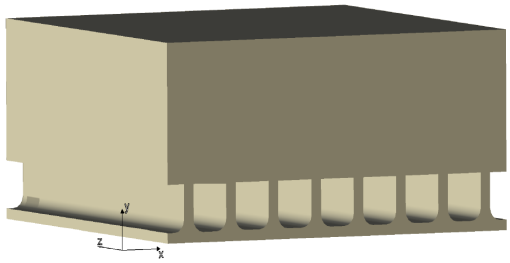

Figure 1 The geometry of system under investigation: a layer with parallel micro-walls connected with a terminal thin plate.

In this paper, we focus on this last aspect of the problem, and propose a new architecture constituted by a sort of parallel wall-like structures as shown in Fig. fig1, which present very high adhesion when the detachment direction is normal to the walls and can be easily removed by applying a bending moment in a plane parallel to the walls.

2. Formulation

We assume that the system is loaded with an external bending moment in the *x-y* plane and applied to the left edge of the structure (see Figure 2).

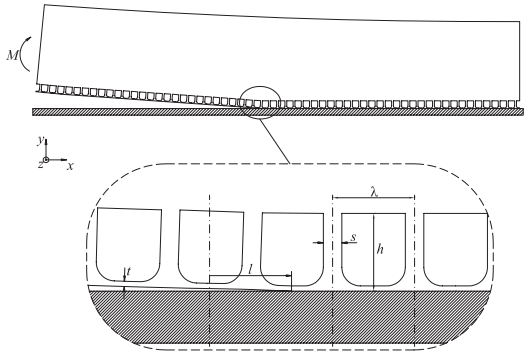

Figure 2 The cross section in the x–y plane of the fibrillar structure under investigation.

The thickness of the backing layer is also assumed significantly larger (up to 10 times) than the fibrils one to correctly reproduce the size of the micro-structure with respect to the supporting layer of a real geometry. The thin film covering the walls makes contact with a rigid flat surface and a crack is assumed extending on the interface along the *x*-direction. We also assume that the structure is much longer (along the *x*-axis) of the existing crack to neglect border effects, and that detachment is governed by the propagation of the crack from the edge.

For a reversible and isothermal transformation the total free energy U_{tot} of the system is the sum of the elastic energy, the potential energy associated to the applied load, and the surface energy U_s. The system will spontaneously moves out of equilibrium when the variation of the total energy U_{tot} is negative, i.e.

$$dU_{tot} = dU_P + dU_{el} + dU_s < 0 \qquad (1)$$

In eq. (1) $dU_P = -Md\theta$ is the variation of the potential energy associated with the constant bending moment $M = K(l)\theta$ (being θ the rotation angle of the left edge of the system where the moment M is applied, and $K(l)$ the constant of proportionality between these two quantities, i.e. the stiffness), $dU_{el} = 1/2Md\theta$ is the change in the elastic energy stored in the system and $dU_s = \Delta\gamma bdl$ is the change in the surface energy, where $\Delta\gamma$ is the work of adhesion. Recalling that the energy release rate G at the crack tip is defined as [18]

$$G = -\frac{\partial(U_{tot} - U_s)}{\partial A} \qquad (2)$$

where $A = bl$ is the detached area (with b the constant linear size of the system along the y -axis,

and l the crack length), spontaneous evolution of the system will occur when

$$dU_{tot} = -(G - \Delta\gamma) b dl \le 0 \qquad (3)$$

If $G > \Delta\gamma$ the above inequality (dF) requires $dl > 0$ and the crack will spontaneously advance causing the detachment of the system. If $G < \Delta\gamma$ the crack should recede. We observe that the strain energy release rate G can be written as

$$G(l) = \frac{M^2}{2b}\frac{\partial C}{\partial l} \qquad (4)$$

Thus, under constant applied bending moment M the quantity G is related to the variation of the system compliance $C = 1/K$, which occurs as the crack advances of a unit length. When the crack moves perpendicularly to the walls, *i.e.* along the x-axis, the periodic geometry of the system will force the energy release rate G to vary periodically with the spatial period λ. Recalling that $\Delta U_{el} = -1/2 \Delta U_P$, the average value of $G(l)$ is then

$$G_{ave} = \frac{\Delta U_{el}}{b\lambda} \qquad (5)$$

where ΔU_{el} is the change in stored elastic energy which occurs when the crack advances of a spacial period λ. On the other hand when the crack moves parallel to the walls, *i.e.* along the y-axis, the energy release rate $G(l)$ cannot change and therefore it remains constant.

A Finite Element (FE) analysis has been carried out, with the aid of the commercial software ANSYS [19], to evaluate the variation in energy release rate which occurs during the crack propagation. Two-dimensional quadratic plane strain elements have been adopted to mesh the overall geometry. The material is assumed to be nearly incompressible with Poisson's ratio $\nu = 0.5$ and elastic modulus $E = 3$ MPa.

3. Results and discussion

Figure 3 shows the variation of the ratio G/G_{flat} between the energy release rate G of the proposed microstructured system and the energy release rate G_{flat} of the flat control sample, as a function of the dimensionless crack length l/λ, for different values of the geometrical parameters. As expected G/G_{flat} is a periodic function of l/λ. The variation of G with the crack length l is positive ($dG/dl > 0$) when the crack is located underneath the wall. In this case energy flows from the system to the crack tip, and the crack tends to spontaneously advance. On the other hand, when the crack tip is in between two adjacent walls, crack trapping (i.e. $dG/dl < 0$) occurs: the crack stops and cannot propagate thus enhancing the adhesive strength, in agreement with some experimental observations [20] and other previous calculations [21].

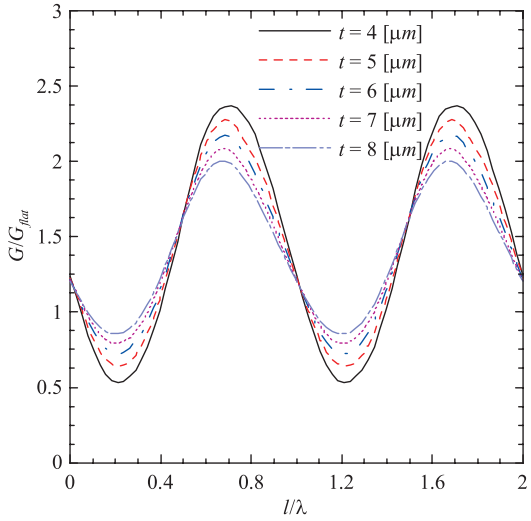

(a)

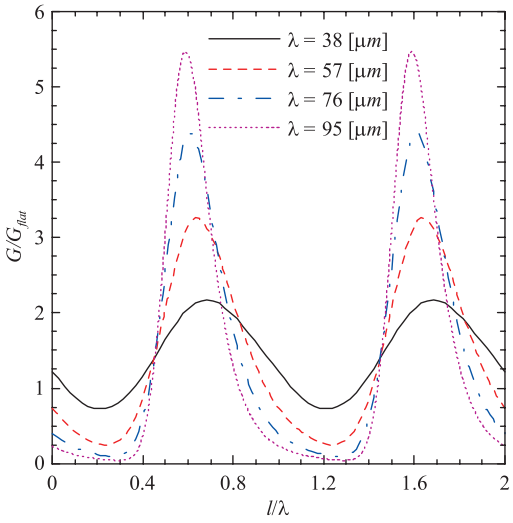

(b)

Figure 3 The variation in the energy-release rate G of the proposed system, normalized with respect to that of a flat control sample G_{flat}, as a function of the dimensionless crack length l/λ.

Notice that the maximum value of G occurs when the crack tip is located below the wall, where the stiffness of the system is higher. This means that crack trapping may occur only in those regions where the system is sufficiently compliant, i.e. in between two consecutive walls. The limiting case is obtained when the thin film covering the walls is interrupted. This should provide the structure with amazing crack tapping properties as already observed in microstructures based on a similar principles, as those constituted by a regular distribution of mushroom shaped pillars [5, 6, 22, 23]. In Figure 3 we also analyze the influence of the thickness t of the thin film, and the spacing λ between the walls on the adhesive properties of the system. Since crack propagation occurs without interruption only when $G_{\min} > \Delta\gamma$, one concludes that those particular modifications of the geometry which determine an increase of the system compliance in between two

adjacent walls, as for example a reduction of t, or rather an increase of λ, are strongly beneficial since they lead to a significant reduction of the minimum value $G_{\min}$ of the energy release rate (i.e. to an enhancement of the crack trapping properties of the structure).

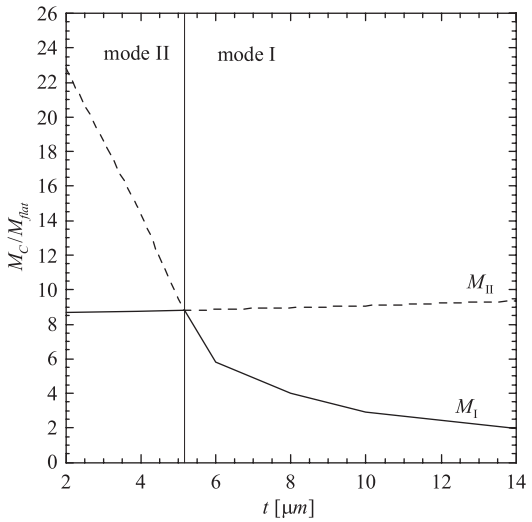

(a)

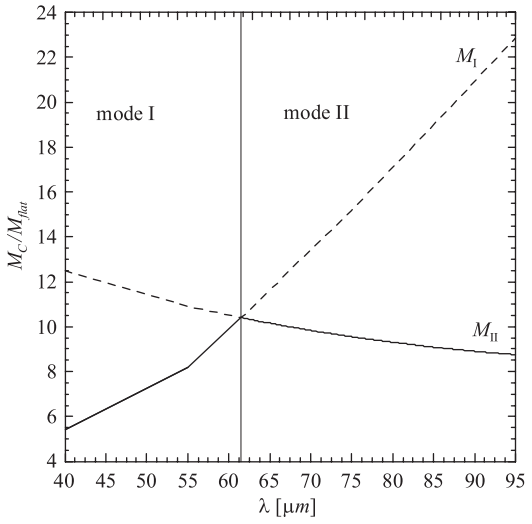

(b)

Figure 4 The variation of the critical bending moment M_C, necessary to fully detach the fibrillar structure, normalized with respect to that of a flat control sample M_{flat}, as a function of the film thickness t with s = 4μm, h = 85μm, λ = 95μm, (a); and wall spacing λ with t = 2μm, s = 4μm, h = 85μm, (b).

In view of the above arguments one concludes, for example, that if the thickness t of the film becomes vanishingly small, the minimum $G_{\min}$ of the energy release rate also vanishes and crack propagation is completely inhibited. In this case, a very high applied moment M would be necessary to detach the system. In reality, by increasing M, large tensile stresses develop beneath the walls and the interface fails because either the so called mode II debonding mechanism is activated (as observed in the case of optimally designed mushroom shaped pillars [5, 6, 23], or in the case where there is a continuous thin sheet connecting the ends of the fibrils [20]), or mode III detachment occurs since the stress beneath the walls exceeds the interfacial van der Walls strength (notice that in the current context, mode I, II, and III do not correspond to the terminology usually adopted in the linear elastic fracture mechanics (LEFM). Here, mode I means an opening mode crack, mode II means interfacial cavitation at a defect, and mode III means full interfacial failure at the theoretical limit, corresponding to the interfacial van der Walls strength).

By following the same procedure as in [5], we can estimate the critical wall stress which activates the mode II debonding mechanism as

$$\sigma_{II} = \left(\frac{\Delta\gamma E^*}{2\pi b a} \right)^{1/2} \qquad (6)$$

where $2a$ is the defect size and $E^* = E/\left(1-\nu^2\right)$ is the composite Young's modulus. Assuming $2a = 20$ nm and $\Delta\gamma = 16\text{mJ/m}^2$, $E = 3\text{MPa}$, $\nu = 0.5$ we get $\sigma_{II} \approx 3.17$ MPa. We notice that, for soft adhesives, the stress σ_{II} is always much less than the theoretical van der Waals contact strength $\sigma_{III} = \Delta\gamma/\rho$, where $\rho \approx 1$nm is the typical range of van der Waals forces. One can easily calculate the bending moment M_I which activates crack propagation from the edge (i.e. mode I debonding mechanism) by enforcing the condition $G_{\min} = \Delta\gamma$, and using Eq. (4), which gives

$$M_I = \sqrt{\frac{2\Delta\gamma b}{\partial C/\partial l\big|_{\min}}}. \qquad (7)$$

Recalling that the system is linearly elastic, the moment M_{II} necessary to activate the mode II debonding mechanism, associated with the growth of interfacial defects underneath the walls, can be calculated as

$$\frac{M_{II}}{M} = \frac{\sigma_{II}}{\sigma}. \qquad (8)$$

where M is the value of the applied moment and σ is the corresponding stress in the walls.

Figure 4 shows the critical bending moment $M_C = \min\{M_I, M_{II}\}$ necessary to fully detach the fibrillar structure as a function of film thickness t, and wall spacing λ. Results are normalized with respect to the debonding moment M_{flat} necessary to detach the flat control sample. Notice, that thanks to the crack trapping properties of the fibrillar structure, the adhesion strength, for the test cases considered in the present study, is increased up to about 10 times if compared to the flat control case. We observe that mode I or mode II debonding may be both activated, depending on the geometry of the system. Therefore it is not beneficial to increase M_I beyond the value M_{II} since, in this case, the mode II debonding mechanism is the one which limits the performance of the system, i.e. the optimal geometry maximizes M_C subjected to the constraint $M_I = M_{II}$. Figure 5 shows the critical ratio M_C/M_{flat} necessary to fully

detach the system as a function of the film thickness t, when the fibrillar structure is loaded in the yz plane, so that crack propagation occurs parallel to the wall-like structures. This time M_C is reduced of more than 10 times if compared to the values obtained in Figure 4.

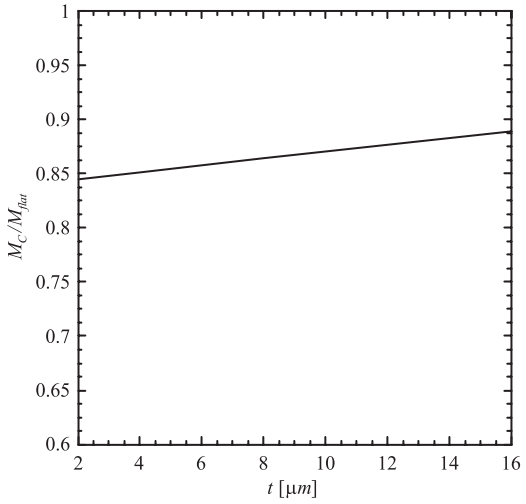

Figure5 The variation of the critical bending moment M_C ,necessary to fully detach the fibrillar structure (this time the detachment direction is parallel to the walls), normalized with respect to that of a flat control sample M_{flat} , as a function of the film thickness t with $s = 4\mu m$, $h = 85\mu m$, $\lambda = 95\mu m$.

The system can be very easily detached, even easier than the flat control sample.

4. Conclusions

In this work we have presented a new architecture for biomimetic micro-structured adhesives which possesses anisotropic adhesion properties. The proposed system is constituted by micro-walls covered by a thin layer, and presents high debonding strength when detachment occurs normally to the micro-walls, whereas it is very easy to detach when detachment occurs parallel to the micro-walls. The reason of such strong adhesion anisotropy is easily explained: In the former case the microstructure enables crack trapping, thus preventing crack propagation. In the latter case crack trapping cannot occur and a crack may easily propagate fed by a constant flux of energy per unit area from the system. The new architecture proposed in this paper, if compared to other structures made of a regular pattern of pillars, may turn out very successful in those applications as manipulation systems, mobile-robots, climbing gloves and suits where anisotropic adhesion is required to prevent the system from remaining stuck to the substrate.

5. References

[1] R. Spolenak, S. Gorb, H. J. Gao, E. Arzt, Proc. R. Soc. London Ser. A, 2005, 461, 305-319.

[2] A. K. Geim, S. V. Dubonos, I. V. Grigorieva, K. S. Novoselov, A. A. Zhukov, S. Y. Shapoval, Nat. Mater., 2003, 2, 461-463.

[3] A. del Campo, C. Greiner, E. Artz, Langmuir, 2007, 23, 10235-10243.

[4] J. Y. Chung, M. K. Chaudhury, J. R. Soc. Interface, 2005, 2, 55-61.

[5] G. Carbone, E. Pierro, N. Gorb, Soft Matter, 2011, 7, 5545-5552.

[6] G. Carbone, E. Pierro, SMALL,2012, 8(9), 1449-1454.

[7] L. Afferrante, G. Carbone, J. Phys.: Condens. Matter, 2010, 22, no. 325107.

[8] J. M. Karp and R. Langer, Nature, 2011, 477, 42-43.

[9] M. K. Kwak, H.-E. Jeong , K. Y. Suh, Adv. Mater., 2011, 23 (34), 3949-3953.

[10] J. Krahn, Y. Liu, A. Sadeghi and C. Menon, Smart Mater. Struct., 2011, 20, 115021.

[11] D. Voigt, A. Karguth, S. Gorb, Shoe soles for the gripping robot: Searching for polymer-based materials maximising friction, Robotics and Autonomous Systems, 60 (8), 1046--1055, (2012)

[12] C. Majidi, R.E. Groff, Y. Maeno, B. Schubert, S. Baek, B. Bush, R. Maboudian, N. Gravish, M. Wilkinson, K. Autumn, R.S. Fearing, Physical Review Letters, 2006. 97, no. 076103.

[13] N. M. Pugno, Nanotoday, 2008, 3, 35-41.

[14] D. Campolo, S. D. Jones, R. S. Fearing, Nanotech., IEEE-Nano Third IEEE Conf., 2003, 2, 856--859.

[15] N. J. Glassmaker, A. Jagota, C.-Y. Hui, J. Kim, J. R. Soc. Interface, 2004, 1, 23-33.

[16] C.-Y. Hui, N. J. Glassmaker, T. Tang, A. Jagota, J. R. Soc. Interface, 2004, 1, 35-48.

[17] A. Peressadko, S. Gorb, J. Adhesion, 2004, 80, 247--261.

[18] D. Maugis, Contact, Adhesion and Rupture of Elastic Solids, Springer Series in Solid State Sciences, Springer-Verlag, Berlin, Heidlberg, New-York, 1999.

[19] ANSYS, ANSYS User's Manual, Version 11.0.

[20] GlassmakerPNAS2007 : N. J. Glassmaker, A. Jagota, C.-Y. Hui, W. L. Noderer, M. K. Chaudhury, PNAS, 2007, 104 (26), 10786-10791.

[21] Kendall1975 : K. Kendall, Proc. R. Soc. A, 1975, 341, 409--428.

[22] Gorbetal2007 : S. Gorb, M. Varenberg, A. Peressadko, J. Tuma, J. R. Soc. Interface, 2007, 4, 271--275.

[23] VarenbergGorb2008 : M. Varenberg, S. Gorb, J. R. Soc. Interface, 2008, 5, 785-789.